

## Article

# Screening and Testing of Anti-Slagging Agents for Tobacco-Stalk-Based Biomass Pellet Fuel for Tobacco Curing

Liang Wang <sup>1</sup>, Yikuan Fan <sup>2</sup>, Fan He <sup>1</sup>, Baoquan Niu <sup>2</sup>, Fengjie Wei <sup>2</sup>, Haobin Zhao <sup>2</sup> and Jianan Wang <sup>1,\*</sup><sup>1</sup> College of Tobacco Science, Henan Agricultural University, Zhengzhou 450002, China<sup>2</sup> China National Tobacco Corporation Henan Provincial Company, Zhengzhou 450046, China

\* Correspondence: wangja@henau.edu.cn; Tel.: +86-371-6355-5763

**Abstract:** Using tobacco stalks as a biomass fuel for flue-cured tobacco production creates a closed, green production cycle. Tobacco stalks are rich in cellulose and can be crushed to produce biomass pellet fuel (BPF). However, single flue-cured tobacco stalk (FCTs) BPF can easily slag during flue-cured tobacco heating (FTH), which affects the operation of biomass burners. In this study, five anti-slagging agents (ASAs), one organic (sodium carboxymethyl cellulose, CMC) and four inorganic (kaolin, KLN; diatomite earth, DTE; calcium carbonate, CCO; and calcium dihydrogen phosphate, CHO), were compared. An ash fusibility test was conducted in two steps to optimize the proportion and treatments that were then screened using FTH. Compared with pure FCT-based BPFs, the slag resistance of 2% CCO and CHO could be controlled below 15%. The emission of particulate matter from chimneys burning BPF with 2% CCO was lower than that with other ASAs. The ASAs achieved complete combustion with low carbon monoxide content in the tail gas. Considering the anti-slagging effect and economic cost, 2% CCO was the best additive for the biomass burner. These results provide a reference for FCT-based BPF production.



**Citation:** Wang, L.; Fan, Y.; He, F.; Niu, B.; Wei, F.; Zhao, H.; Wang, J. Screening and Testing of Anti-Slagging Agents for Tobacco-Stalk-Based Biomass Pellet Fuel for Tobacco Curing. *Processes* **2022**, *10*, 1690. <https://doi.org/10.3390/pr10091690>

Academic Editors: Zhicheng Jiang, Yuhe Liao and Aneta Magdziarz

Received: 22 July 2022

Accepted: 23 August 2022

Published: 25 August 2022

**Publisher's Note:** MDPI stays neutral with regard to jurisdictional claims in published maps and institutional affiliations.



**Copyright:** © 2022 by the authors. Licensee MDPI, Basel, Switzerland. This article is an open access article distributed under the terms and conditions of the Creative Commons Attribution (CC BY) license (<https://creativecommons.org/licenses/by/4.0/>).

**Keywords:** circular agriculture; green energy; tobacco stalk; pellet fuel; anti-coking; tobacco curing

## 1. Introduction

Biomass pellet fuel (BPF) is processed from agricultural and forestry waste. Bypassing the use of coal-fired heating for flue-cured tobacco curing can effectively ameliorate the current global environmental pollution problem [1]. With technological advances increasing the use of combustion technology using BPF burners for flue-cured tobacco heating (FTH), a growing number of flue-cured-tobacco-producing countries and regions have begun to transition from fossil fuels to biomass fuel as their primary tobacco-curing heat source [2,3]. Through the analysis of various heat sources in the agricultural field of flue-cured tobacco production, previous studies have indicated that BPT offers an optimal method to realize the green production of flue-cured tobacco [4–6].

After tobacco leaves are harvested, the flue-cured tobacco stalks (FCTs) are an important source of BPF production in tobacco-cultivating areas [7]. As the largest producer of flue-cured tobacco globally, China's annual output of FCTs is approximately 1.8 million tons [8]. BPFs made by FCT heating can contribute to the development of a closed-loop system in agricultural tobacco production [9]. The heat storage ability of a 3 hm<sup>2</sup> tobacco field of FCTs can meet the heat requirement for the curing of 1 hm<sup>2</sup> of tobacco curing. This also provides an endpoint for the tobacco stalk waste produced after retrieval of the crop from the field [10,11]. However, the lower content of Si and Fe in FCTs evidently differs from that in general crop straw and forest residue [12]. It is also an important factor for the slagging of FCT-based BPFs in the heating process of tobacco curing. The control methods for reducing the slagging problem of BDF include mixed burning, washing or adding additives. Mixed burning may introduce new pollution sources and may even require the consideration of the introduction of new exhaust gas treatment devices [13]. If

the waste water produced in the process of washing is not properly treated, it can easily cause secondary dyeing [14]. The method of adding additives has good applicability because it is easy to operate and has minimal effect on the combustion process [15]. Previous studies have adopted a ratio of 15% FCTs and 85% sawdust to achieve better anti-slagging effects [16]. However, regional differences in the distribution of biomass resources can lead to the long-distance transportation of biomass raw materials and a rise in the production cost of granular fuel [17]. Biomass fuel agents could reduce the slagging/fouling potential due to alkali [18]; for instance, industrial boilers often use anti-slagging agents (ASAs) to reduce the slagging problem of BDF in the combustion process. Si et al. reported that the addition of carboxymethyl cellulose (CMC) could effectively enhance the durability, compressive strength and relaxation density of straw and cotton straw formed particles [19]. Mineral additives rich in metal oxides, such as diatomite and kaolin, inhibit ash melting by converting low-melting compounds into high-melting  $KAlSiO_4$  and  $KAlSi_2O$  during fuel combustion [20]. The use of calcium-based additives with the objective of reducing sintering and slagging aims mainly at increasing the melting temperature of the formed silicates and phosphates [21]. Wang et al. investigated the influence of phosphorous-based additives  $Ca(H_2PO_4)_2$  on K fixation and the ash melting behavior of maize straw and corn stalks briquettes with lab tests [22]. To date, there has been no report on the use of ASAs in BPF made from tobacco stalks for FTH. This study investigated the potential of ASAs to reduce slagging in the production of FCT-based BPFs in the process of FTH.

## 2. Materials and Methods

### 2.1. Experimental Setup

The experiment was conducted at the Xuchang campus of Henan Agricultural University, China, at the workshop of Xuchang Tongxing Modern Agricultural Technology Co., Ltd. (Xuchang, China), and at the Duguan Tobacco Station in Lushi County, Sanmenxia City, China, between 2020 and 2021.

According to methods described in the existing literature [23] and the availability of ASAs, the following ASAs were used in this study: organic ASA—carboxymethyl cellulose (CMC)—and inorganic ASAs—kaolin (KLN), diatomaceous earth (DTE), calcium carbonate (CCO) and calcium dihydrogen phosphate (CHO). Each anti-slagging agent (ASA) was produced by Tianjin Zhiyuan Chemical Reagent Co., Ltd., China. The CMC and CCO was AR, and the KLN and DTE was CP. Due to the increased production cost of ASA, each test treatment was added at 1 wt%, 2 wt% and 3 wt% of FCTs after crushing. The ASA ratios used in the experiments are shown in Table 1.

**Table 1.** Percentage of anti-slagging agents used in the experimental treatments for biomass pellet fuel made from tobacco stalks for flue-cured tobacco heating.

Additive Molecular Formula	Abbreviations	Additive Ratio (wt%)
Pure tobacco stalk	CK	0
$[C_6H_7O_2(OH)_2OCH_2COONa]_n$	CMC 1	1
	CMC 2	2
	CMC 3	3
$Al_2O_3 \cdot 2SiO_2 \cdot 2H_2O$	KLN 1	1
	KLN 2	2
	KLN 3	3
$SiO_2 \cdot nH_2O$	DTE 1	1
	DTE 2	2
	DTE 3	3
$CaCO_3$	CCO 1	1
	CCO 2	2
	CCO 3	3

**Table 1.** *Cont.*

Additive Molecular Formula	Abbreviations	Additive Ratio (wt%)
Ca(H) <sub>2</sub> PO <sub>4</sub>	CHO 1	1
	CHO 2	2
	CHO 3	3

The FCTs used for the experiment were obtained from Yonghui Cooperative of Sheqi County, Nanyang City, Henan Province, China. The chamber electric furnace (SX2-10-12N, Shanghai Yiheng Scientific Instrument Co., Ltd.) was used to test characterization. The element analyzer (VARIO EL III, ELEMENTAR Co., Ltd., Germany) was used to test the elemental analysis. The characterization and conventional analysis are shown in Table 2. A low heating value (LHV) of 14.87 MJ·kg<sup>-1</sup> for the FCT testing machine, a calorimeter (SDC712, Hunan Sande Technology Co., Ltd.), was used, which complied with the GB/T 30727-2014 Chinese measurement standard.

**Table 2.** Characterization and elemental analysis of tobacco stalk.

Characterization/wt%				Elemental Analysis/wt%					LHV/MJ·kg <sup>-1</sup>
Water Content	Ash	Volatile Matter	Fixed Carbon	C	H	O	N	S	
7.20	18.99	57.91	15.90	37.70	5.31	55.24	1.57	0.18	14.87

LHV, low heating value (MJ·kg<sup>-1</sup>); wt%, % of dry weight.

## 2.2. Experimental Methods

### 2.2.1. Screening Steps

This study was divided into a laboratory screening test and an outdoor detection test. First, the indoor ash fusibility characteristic index was employed to judge the additive reference of different experimental treatments, and the most appropriate proportion of ASA was selected. The production of outdoor BPF was organized for different treatments following screening. Finally, a chimney tail gas detection, slagging and economic feasibility analysis were conducted during the FCT process. The particle size of BPF was unified at 10 mm, which is used in most tobacco-planting areas in China.

### 2.2.2. Test Sample Preparation

Laboratory sample preparation: The retrieved FCTs were air dried under natural conditions, and raw materials less than 0.6 mm were crushed and screened using a small pulverizer. Different ASAs were screened using a 200-mesh screen before addition. After uniform mixing of the two substances, the prepared, mixed raw materials were precisely weighed to 2.5 ± 0.1 g, and a microcomputer-controlled electronic universal testing machine (HD-B615A-S, Xiamen Haida Precision Instrument Co., Ltd., Xiamen, China) was used to compress the mixed raw materials. The compression rod rate was 20 mm/min. When the specified pressure of the rod achieved 45 kN, the compression was stopped, and the pressure was maintained for 3 min. Finally, a demolding rate of 5 mm/min was used to obtain BPF.

Outdoor sample preparation method: The Nanyang Sheqi BPF processing plant was used for FCT-based BPF production. The economic cost of adding various ASAs to BPF production was calculated.

### 2.2.3. Ash Fusibility Test

The ash fusion point determination meter (BYTHR-9F, Hebi Boyuntian Technology Co., Ltd., Zhengzhou, China) was used to test the four characteristics of the morphological changes in the ash cone. The ash sample of the different burn treatments was molded into a regular triangular cone with a height of 20 mm and a length of 7 mm at the bottom and was

then placed into a reducing atmosphere containing hydrogen. The temperature was raised to 700 °C at 15 °C/min, then to 900 °C at 10 °C/min and finally to 1500 °C at 5 °C/min. The four characteristics of the morphological changes in the ash cone, including deformation temperature (DT), softening temperature (ST), hemispherical temperature (HT) and flow temperature (FT), were observed and recorded as the temperature increased [24]. A total of 16 treatments, or 64 temperature measurement points, needed to be tested.

#### 2.2.4. Chimney Emission Detection

The burner, which was recommended by the State Tobacco Monopoly Administration in China [3], was inserted into the original, coal-fired heating equipment following the removal of bars and insulated linings (Figure 1). The exhaust port at the tail of the chimney was used as the detection port for tail gas.

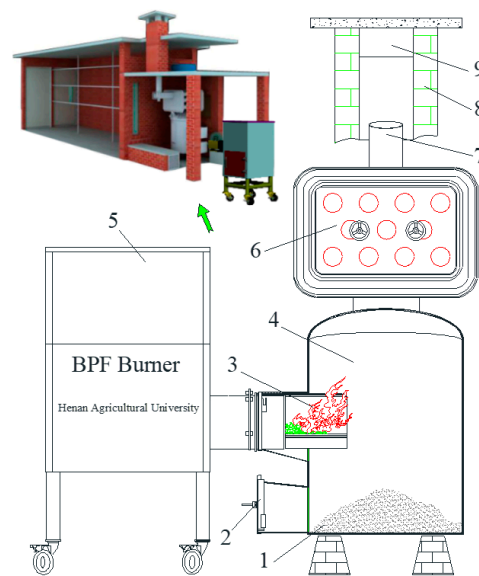


**Figure 1.** Flowchart of the biomass combustion test in tobacco-heating equipment: 1. piled ash; 2. ash-clearing door; 3. furnace; 4. combustion chamber for heating tobacco; 5. pellet box of burner; 6. radiator; 7. gas exhaust port of radiator; 8. chimney of bulk curing barn; 9. sampling port.

The flue gas sampler monitored the chimney after 15 min of the ignition of the burners in order to keep the same working conditions. The low concentration gas tester (TW-3200D/SYYQ-164, Qingdao Tuowei Intelligent Instrument Co., Ltd., Qingdao, China) and the dual flue gas sampler (WT-2610/SYYQ-103, Qingdao Tuowei Zhineng Instrument Co., Ltd., Qingdao, China) were employed for collecting gas. A gas chromatography–mass spectrometer (Agilent 8890, Agilent Technology (China) Co., Ltd.) was used to detect the type and content of tail gas collected by the vacuum box sampler during tobacco curing and heating.

#### 2.2.5. Slagging in the Flue-Cured Tobacco Heating Process

The slag discharge system of the biomass burner was opened. Under the mode of FTH, relying on the slag removal system of the biomass burner, 100 kg BPF produced by each treatment was placed into the pellet box of the burner for combustion. The ash by the push rod of the burner was pushed into the ash pool at the lower part of the coal-fired equipment. After cooling, all bottom ash was removed and cleaned. According to the GB/T 1512-2001 method for determining the slagging property of coal, the slagging rate of the bottom ash of each treatment was calculated using Equation (1):

$$C_{lin} = G_1/G \times 100\% \quad (1)$$

where  $C_{lin}$  is the slagging rate, %;  $G_1$  is the mass of slag block with a particle size greater than 6 mm and  $G$  is the mass of total ash, g.

### 2.2.6. Natural Ash Slagging

The slag discharge system of the biomass burner was closed. After 100 kg of BPF was burned in the outdoor air, the slagging of each treated furnace was photographed using a mobile phone (Huawei P10, Huawei Technology Co., Ltd., Shenzhen, China). These photos are presented in Figure 2.

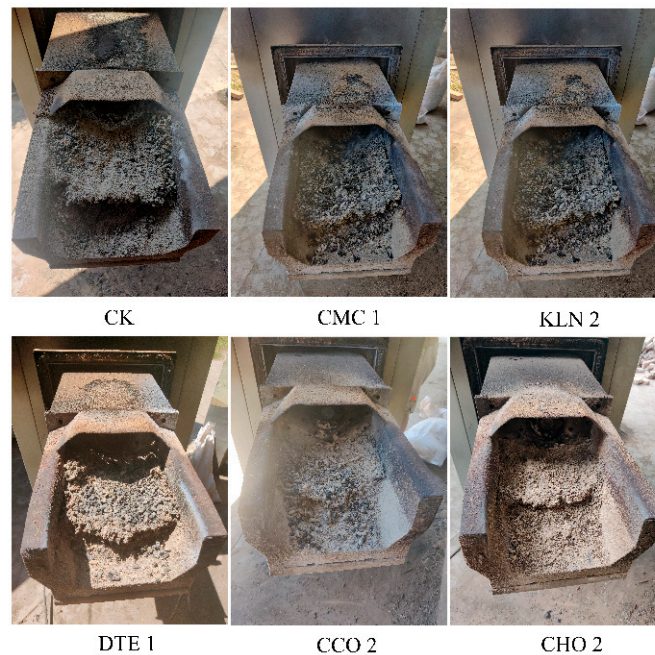


**Figure 2.** Comparison of furnace slagging under natural ventilation: calcium carbonate (CCO), calcium dihydrogen phosphate (CHO), carboxymethyl cellulose (CMC), control (CK), diatomaceous earth (DTE) and kaolin (KLN).

### 2.2.7. Data Processing

The AutoCAD 2013 software (Autodesk, Inc., San Rafael, CA, USA) was used to draw the structure diagram of the biomass burner and coal-fired furnace. The picture is presented in Figure 1. GraphPad Prism v5.0 (U.S. GraphPad Software Company) was used for data analysis and automatic image generation. The related data analysis and automatic image generation are presented in Figure 3.

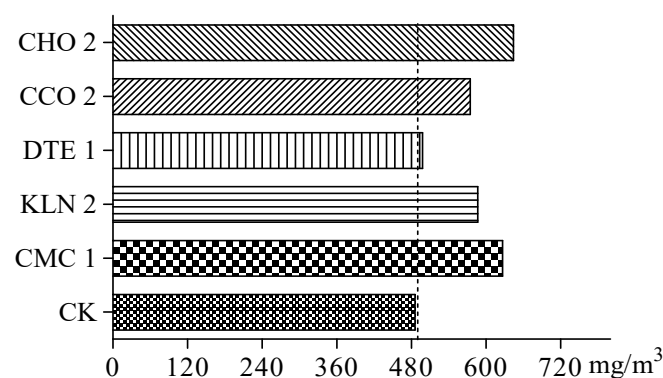


**Figure 3.** Particulate matter content from the chimney tail exhaust: calcium carbonate (CCO), calcium dihydrogen phosphate (CHO), carboxymethyl cellulose (CMC), control (CK), diatomaceous earth (DTE) and kaolin (KLN).

### 3. Results

#### 3.1. Effects of Different Additive Ratios on the Ash Fusibility of the Biomass Pellet Fuel

When different ASA ratios were added to the crushed FCTs, BPF ash fusibility demonstrated three key patterns: (1) the ST of CCO and CHO molding fuel gradually increased with an increase in ASA content; (2) KLN particulate fuel initially decreased and then increased; and (3) CMC and DTE reduced the ST of formed fuel and CMC decreased with an increase in additive content (Table 3). However, compared with the FCTs, DTE reduced at almost 80 °C. A maximum difference was observed between CCO 2 and KLN 1 at 60 °C. CMC 3, KLN 1, DTE 1, DTE 2 and CHO 3 had a minimum difference of 10 °C. Due to the large difference between the content of some components in biomass ash and coal ash, ST was deemed unsuitable for use due to the judgment index of biomass slagging. Previous studies used the difference between ST and DT as a reference. The large difference is conducive to reducing the slagging inclination of briquette fuel [25,26]. Combined with the environment of heating flue-cured tobacco with biomass fuel [27], CMC 1, KLN 2, DTE 1, CCO 2 and CHO 2 were preliminarily selected for the next step of the BPF production test.

**Table 3.** Ash melting point of granular fuel with different additives (°C).

Controls	DT	ST	HT	FT
CK	1260	1270	1290	1300
CMC 1	1220	1260	1270	1300
CMC 2	1210	1250	1260	1280
CMC 3	1230	1240	1260	1270
KLN 1	1180	1190	1200	1220
KLN 2	1160	1220	1230	1250
KLN 3	1290	1330	1350	1390
DTE 1	1170	1190	1200	1240
DTE 2	1180	1190	1200	1210
DTE 3	1180	1190	1210	1220
CCO 1	1230	1280	1300	1350
CCO 2	1260	1320	1330	1340
CCO 3	1290	1330	1350	1380
CHO 1	1280	1300	1310	1320
CHO 2	1280	1320	1330	1340
CHO 3	1370	1380	1390	1400

Calcium carbonate (CCO), carboxymethyl cellulose (CMC), calcium dihydrogen phosphate (CHO), diatomaceous earth (DTE), deformation temperature (DT), flow temperature (FT), hemi-spherical temperature (HT) and kaolin (KLN).

The characterization and LHV of the optimized test treatment is shown in Table 4. The results show that the addition of additives had no effect on the fuel moisture, ash and volatile matter. Inorganic ASA KLN 2 and DTE 1 both improved the LHV of granular fuel after FCT molding. Moreover, DTE 1 increased LHV by 9%. Furthermore, CCO 2 and CHO 2 reduced the low calorific value. The difference in the data of the low heat value of pure tobacco sticks and the five additives in Table 2 in the manuscript is between −0.39~1.22%, which is very reasonable compared to ±3% recommended by Yuan et al. [28].

**Table 4.** Industrial analysis and low heat value (LHV) of test treatment after screening.

Additive Type	Characterization/wt%				LHV/MJ·kg <sup>-1</sup>
	Water Content	Ash	Volatile Matter	Fixed Carbon	
CMC 1	7.83	19.03	56.57	16.30	16.09
KLN 2	7.58	18.31	58.98	15.13	16.02
DTE 1	7.51	19.89	58.30	14.30	16.21
CCO 2	7.15	20.90	56.63	15.32	14.65
CHO 2	6.89	20.01	58.20	14.90	14.48

Calcium carbonate (CCO), carboxymethyl cellulose (CMC), calcium dihydrogen phosphate (CHO), diatomaceous earth (DTE) and kaolin (KLN); wt%, % of dry weight.

### 3.2. Comparison of Slagging in the Flue-Cured Tobacco Heating Process

Table 5 shows the statistical comparison of the slagging rate of different treatments in the environment of FTH. Compared with CK, the different experimental treatments exhibited a certain slagging resistance. Overall, the order (most to least) of the ASA effect was: CHO 2 > CCO 2 > KLN 2 > DTE 1 > CMC 1. CHO 2 had the best anti-slagging effect, controlling the slagging rate by 10.14% and reducing it by 36.54%.

**Table 5.** Slagging rate of bottom ash under controlled conditions.

Controls	Total Ash (kg)	Ash Block (kg)	Slagging Rate (%)
CK	4.50	2.10	46.70
CMC 1	4.71	1.50	36.60
KLN 2	4.93	1.00	20.28
DTE 1	4.60	1.30	28.20
CCO 2	5.01	0.70	13.97
CHO 2	4.93	0.50	10.14

Calcium carbonate (CCO), calcium dihydrogen phosphate (CHO), carboxymethyl cellulose (CMC), control (CK), diatomaceous earth (DTE) and kaolin (KLN).

Figure 2 shows the slagging of different BPFs controlled by the natural ash slagging mode. Overall, the slagging of CCO 2 and CHO 2 furnaces was lower than as assessed visually (unaided). Bottom ash slagging was similar to that of CMC 1, KLN 2 and DTE 2 during the FTH process.

### 3.3. Analysis of Particulate Matter Emission from the Chimney

Compared with CK, the particles discharged from the chimney increased by varying degrees after adding different ASAs (Figure 3), with an increase of 2.47–32.51%. The order of emission levels (least to most) from ASA addition was: DTE 1 < CCO 2 < KLN 2 < CMC 1 < CHO 2.

### 3.4. Type and Content of Gas Discharged from the Chimney

The two gas detection instruments can detect gases such as fluoride, benzene series and phenolic compounds (Table 6). In the process of FTH, benzene series, phenolic compounds, formaldehyde and benzoapyrene were not detected. CMC 1 reduced the nitric oxide (NO) emissions of burned BPF, which may be because adding organic CMC 1 can improve the particle condensation of BPF and reduce NO emissions from fuel. Other inorganic additives can reduce the CO emissions from FCT-based BPF, excluding the high content of CO after the combustion of organic additive CMC 1.

**Table 6.** Detection of gas discharged from the chimney (mg/m<sup>3</sup>).

	CK	CMC 1	KLN 2	DTE 1	CCO 2	CHO 2
Fluoride	0.13	0.18	0.16	0.13	0.09	0.08
Benzene series	-	-	-	-	-	-
Phenolic compounds	-	-	-	-	-	-
Hydrogen sulfide	-	0.02	0.03	-	0.02	0.02
Formaldehyde	-	-	-	-	-	-
Chlorine	1.70	-	-	3.40	-	-
Ammonia	1.96	1.12	0.47	0.68	0.70	1.87
Asphalt smoke	-	-	-	0.50	0.40	0.50
Non-methane hydrocarbons	9.15	9.40	6.05	4.32	5.80	5.10
Benzoapyrene	-	-	-	-	-	-
Hydrogen chloride	1.60	0.90	1.10	2.30	1.40	0.70
Oxygen (O <sub>2</sub> )	13.45	15.79	12.99	10.44	11.01	12.71
Sulfur dioxide (SO <sub>2</sub> )	66.40	11.30	101.40	207.40	130.20	197.50
Nitric oxide (NO)	237.00	200.60	245.90	310.50	502.70	344.40
Nitrogen oxides (NOX)	362.60	307.70	349.50	274.70	447.10	306.50
Carbon monoxide (CO)	184.00	480.00	169.90	177.10	174.50	176.10

Note: “-” means not detected; calcium carbonate (CCO), calcium dihydrogen phosphate (CHO), carboxymethyl cellulose (CMC), control (CK), diatomaceous earth (DTE) and kaolin (KLN).

Table 6 shows large values for carbon monoxide (CO) in all cases. Usually, such a value indicates insufficient air (oxygen) supply to the combustion chamber and insufficient utilization of material for combustion purposes [29]. It shows that the ventilation in the air supply system of the BPF burner used in this experiment needs to be increased in the future to promote the full combustion of BPF.

### 3.5. Comparative Analysis of Production Cost

Table 7 shows the production cost of BPF with different additives. The order of increasing costs was CMC 1 > CHO 2 > KLN 2 > DTE 1 > CCO 2. CHO 2 exhibited the best anti-slagging effect; however, the cost was higher than CCO 2. The cost of CCO 2 was 1.85 USD/t and possessed the lowest increase cost; therefore, it could meet the demand for FTH. Considering the cost and anti-slagging effect, CCO 2 resulted in superior anti-slagging performance with the lowest cost.

**Table 7.** Cost comparison of different additives (USD/t).

	Market Price	Increase Cost
CMC 1	2374.24	23.51
KLN 2	316.57	6.14
DTE 1	474.85	4.70
CCO 2	94.97	1.85
CHO 2	474.85	9.22

Calcium carbonate (CCO), calcium dihydrogen phosphate (CHO), carboxymethyl cellulose (CMC), control (CK), diatomaceous earth (DTE) and kaolin (KLN).

## 4. Discussion

Under the condition of FTH, FCTs added to ASA can reduce emissions from chimney particles by varying degrees. Previous research has determined that increasing the potassium content of BPT can reduce the emissions of particulate matter, and the increase is positively correlated with the reduction [30]. This may explain the increase in particulate matter emission after adding ASA to each treatment. Some silicon-rich mineral additives can capture volatile elements produced during combustion and are often used to reduce particulate matter emissions related to ash [31]. The addition of DTE can increase Si content in FCT fuel and can reduce the emission of particulate matter in chimney tail gas compared with other treatments. However, the anti-slagging effect is poor.

Spherical particles burning pure FCTs are mainly composed of potassium and silicon [32]. Calcium-based additives in corps straw can introduce calcium into molten silicate to form calcium silicate salt with a higher melting point, thus improving the fusibility of ash in normal circumstances [21] of 10% in the boiler. In the study of corn straw by Yuan et al. [28], adding 3% CCO can reduce the slagging rate to less than 10% in the boiler. For FTH, the heating requirements of a standard bulk curing barn in China's tobacco areas is about 2000–20,000 kJ/h [33–35], and during tobacco curing, the temperature of the biomass burner furnace continuously changes between 600 and 1100 °C [27], which are less than the heating capacity and furnace temperature of ordinary boilers. This cross comparison shows that 2% CCO additive is suitable for FCTs for FTH.

In this study, the slagging rate of ash after the combustion of 2% CHO treatments decreased to 10.14%. However, there was a gap when the slagging rate was less than 10% compared with that of Al and Fe additives used by Zhang et al. in a high-temperature, fluidized bed [12]. Therefore, for a wide variety of biomass additives, the use of ASAs for improving slag resistance in tobacco-stalk-based BPFs requires further investigation.

## 5. Conclusions

Five ASAs were added to BPF in different ratios to investigate solutions for the slagging of FCT-based BPFs during FTH. Our results demonstrate that a slag resistance rate of 2% from CHO and CCO treatment could be controlled below 15%, and the fuel was fully burned, thus meeting the demand of flue-cured tobacco heating. Considering the rate of burner ash slagging under the state of flue-cured tobacco curing and the economic cost after ASA addition, 2% CCO was deemed to be the optimal ASA for flue-cured tobacco heating with FCT-based BPFs. This report only studies the effects of five single ASAs for flue-cured tobacco heating with FCT-based BPFs on the slagging and chimney particulate emissions of biomass fuels during the combustion process. Further research is needed on the effects of more additives and composite additives. Moreover, considering that the biomass burner for flue-cured tobacco can only meet the needs of tobacco leaf curing, the effect of anti-slagging agents needs to be further studied when applied to other fields.

**Author Contributions:** Conceptualization, Y.F. and J.W.; methodology, J.W.; software, L.W.; validation, F.W., B.N. and H.Z.; formal analysis, L.W.; investigation, F.H.; resources, J.W.; data curation, L.W.; writing—original draft preparation, L.W.; writing—review and editing, J.W.; visualization, L.W.; supervision, F.H.; project administration, J.W.; funding acquisition, Y.F. All authors have read and agreed to the published version of the manuscript.

**Funding:** This work was funded by the Henan Provincial Tobacco Company (Grant no. 2018410000270097) and China tobacco Henan industrial Co., Ltd. (Grant no. 2022410000340099).

**Data Availability Statement:** The datasets used and/or analyzed during the current study are available from the corresponding author upon reasonable request.

**Conflicts of Interest:** The authors declare no conflict of interest.

## Abbreviations

Anti-slagging agents (ASAs), biomass pellet fuel (BPF), calcium carbonate (CCO), carboxymethyl cellulose (CMC), calcium dihydrogen phosphate (CHO), control (CK), diatomaceous earth (DTE), deformation temperature (DT), flow temperature (FT), flue-cured tobacco heating (FTH), flue-cured tobacco stalk (FCTs), hemispherical temperature (HT), kaolin (KLN), low heating value (LHV), softening temperature (ST).

## References

1. Abosedede, I.A.; Peter, O.A.; Adunola, A.A.T. Biomass valorization: Agricultural waste in environmental protection, phytomedicine and biofuel production. In *Biomass Volume Estimation and Valorization for Energy*; Tumuluru, J.S., Ed.; IntechOpen: London, UK, 2017. [CrossRef]
2. De Farias, J.A.; Schneider, P.R.; Biali, L.J. Diagnosis of the forests planted in river basin of 'Pardo' River, Rio Grande do Sul State. *Cienc. Florest.* **2017**, *27*, 339–352.
3. Song, Z.P.; Wei, F.J.; Su, X.F.; Wang, Y.; Fan, Y.; Wang, J. Application of automatic control furnace for combustion of biomass briquette fuel for tobacco curing. *Therm. Sci.* **2021**, *25*, 2425–2435. [CrossRef]
4. Bortolini, M.; Gamberi, M.; Mora, C.; Regattieri, A. Greening the Tobacco Flue-Curing Process Using Biomass Energy: A feasibility study for the flue-cured Virginia type in Italy. *Int. J. Green Energy* **2019**, *16*, 1220–1229. [CrossRef]
5. Dessbesell, L.; De Farias, J.A.; Roesch, F. Complementing firewood with alternative energy sources in Rio Pardo Watershed, Brazil. *Cienc. Rural.* **2017**, *47*, 1–3. [CrossRef]
6. Wang, J.A.; Fan, Y.K.; Zhao, H.B.; Liu, J.J.; Song, C.P.; Wei, F.J. Performance of biomass fuel pellets of different sizes in combustion heating for tobacco flue-curing. *J. Environ. Prot. Ecol.* **2022**, *23*, 1031–1038.
7. Zhao, D.Q.; Dai, Y.; Feng, G.L.; Yang, J.; Tan, L.L.; Li, J. Chemical composition, fiber morphology and biological structure of tobacco stalks. *Tob. Sci. Technol.* **2016**, *49*, 80–86.
8. Wang, J.A.; Zhang, Q.; Wei, Y.W.; Yang, G.; Wei, F. Integrated furnace for combustion/gasification of biomass fuel for tobacco curing. *Waste Biomass Valor.* **2019**, *10*, 2037–2044. [CrossRef]
9. Barla, F.G.; Kumar, S. Tobacco biomass as a source of advanced biofuels. *Biofuels* **2019**, *10*, 335–346. [CrossRef]
10. Wang, J.A.; Liu, G.S. Development of tobacco-curing system centrally heated by biomass-fueled hot water boiler. *Acta Tabacaria Sin.* **2012**, *18*, 32–37.
11. Zhang, Y.; Pan, Z.; Yang, J.; Chen, J.; Chen, K.; Yan, K.; Meng, X.; Zhang, X.; He, M. Study on the suppression mechanism of (NH<sub>4</sub>)<sub>2</sub>CO<sub>3</sub> and SiC for polyethylene deflagration based on flame propagation and experimental analysis. *Powder Technol.* **2022**, *399*, 1. [CrossRef]
12. Zhang, S.H.; Yang, Z.X.; Wang, X.H.; Chen, H.P. Experiment on agglomeration characteristics during fluidized bed combustion of tobacco stem. *Trans. Chin. Soc. Agric. Mach.* **2012**, *43*, 97–106.
13. Fournel, S.; Palacios, J.H.; Godbout, S.; Heitz, M. Effect of additives and fuel blending on emissions and ash-related problems from small-scale combustion of reed canary grass. *Agriculture* **2015**, *5*, 561–576. [CrossRef]
14. Deng, L.; Zhang, T. Effect of water washing on fuel properties, pyrolysis and combustion characteristics, and ash fusibility of bioma. *Fuel Process. Technol.* **2013**, *106*, 712–720. [CrossRef]
15. Wang, L.; Hustad, J.E.; Skreiberg, Ø.; Skjevrak, G.; Grønli, M. A critical review on additives to reduce ash related operation problems in biomass combustion applications. *Energy Procedia* **2012**, *20*, 20–29. [CrossRef]
16. Qiu, Z.D.; Lian, Y.C.; Lu, Y.; Wang, X.; Lin, M.G.; Lin, Q.T.; Yu, H.; Gu, L.; Zhang, Z.Y. Application of tobacco stem and sawdust formulated biomass fuel in tobacco curing. *J. Fujian Agric. For. Univ.* **2021**, *50*, 10–15.
17. Cheng, W.R.; Zhang, Y.F.; Wang, P. Effect of spatial distribution and number of raw material collection locations on the transportation costs of biomass thermal power plants. *Sustain. Cities Soc.* **2020**, *55*, 102040. [CrossRef]
18. Vamvuka, D.; Zografos, D.; Alevizos, G. Control methods for mitigating biomass ash-related problems in fluidized beds. *Bioresour. Technol.* **2008**, *99*, 3534–3544. [CrossRef]
19. Si, Y.; Hu, J.; Wang, X.; Yang, H.; Chen, Y.; Shao, J. Effect of carboxymethyl cellulose binder on the quality of biomass pellets. *Energy Fuels* **2016**, *30*, 5799–5808. [CrossRef]
20. Niu, Y.; Wang, Z.; Zhu, Y. Experimental evaluation of additives and K<sub>2</sub>O-SiO<sub>2</sub>-Al<sub>2</sub>O<sub>3</sub> diagrams on high temperature silicate melt-induced slagging during biomass combustion. *Fuel* **2016**, *179*, 52–59. [CrossRef]
21. Thy, P.; Leshner, C.E.; Jenkins, B.M. Experimental determination of high-temperature elemental losses from biomass slag. *Fuel* **2000**, *79*, 693–700. [CrossRef]
22. Wang, Q.; Han, K.; Wang, J. Influence of phosphorous based additives on ash melting characteristics during combustion of biomass briquette fuel. *Renew. Energy* **2017**, *113*, 428–437. [CrossRef]
23. Míguez, J.L.; Porteiro, J.; Behrendt, F.; Blanco, D.; Patiño, D.; Dieguez-Alonso, A. Review of the use of additives to mitigate operational problems associated with the combustion of biomass with high content in ash-forming species. *Renew. Sustain. Energy Rev.* **2021**, *141*, 110502. [CrossRef]
24. Zhang, L.; Li, J.; Xue, J.; Zhang, C.; Fang, X. Experimental studies on the changing characteristics of the gas flow capacity on bituminous coal in CO<sub>2</sub>-ECBM and N<sub>2</sub>-ECBM. *Fuel* **2021**, *291*, 120115. [CrossRef]
25. Niu, Y.Q.; Tan, H.Z.; Wang, X.B.; Xu, T.; Liu, Z.; Liu, Y. Fusion characteristics of capsicum stalk ash. *Asia Pac. J. Chem. Eng.* **2011**, *6*, 679–684. [CrossRef]
26. Zhu, Y.M.; Tan, H.Z.; Niu, Y.Q.; Wang, X. Experimental study on ash fusion characteristics and slagging potential using simulated biomass ashes. *J. Energy Inst.* **2019**, *92*, 1889–1896. [CrossRef]
27. Wang, J.A.; Fan, Y.K.; Zhang, T.Q.; Wei, F.J.; Zhao, H.B.; He, L.; Liu, J.J.; Wang, P.F.; Song, C.P. Design and test of biomass furnace in intensive baking room. *Acta Tabacaria Sin.* **2021**, *27*, 111–119.
28. Yuan, Y.W.; Zhao, L.X.; Meng, H.B.; Lin, C.; Tian, Y.S. Effects comparison on anti-slagging additives of corn straw biomass pellet fuel. *Trans. CSAE* **2010**, *11*, 251–255. (In Chinese)

29. Rahman, M.A.; Hopke, P.K. Mechanistic pathway of carbon monoxide off-gassing from wood pellets. *Energy Fuels* **2016**, *30*, 5809–5815. [[CrossRef](#)]
30. Zeng, T.; Weller, N.; Pollex, A.; Lenz, V. Blended biomass pellets as fuel for small scale combustion appliances: Influence on gaseous and total particulate matter emissions and applicability of fuel indices. *Fuel* **2016**, *184*, 689–700. [[CrossRef](#)]
31. Han, J.K.; Yu, D.X.; Wu, J.Q.; Yu, X.; Liu, F.; Wang, J.; Xu, M. Fine ash formation and slagging deposition during combustion of silicon-rich biomasses and their blends with a low-rank coal. *Energy Fuels* **2019**, *33*, 5875–5882. [[CrossRef](#)]
32. Ma, X.Q.; Luo, Z.Y.; Fang, M.X.; Yu, C.J.; Cen, K.F. Effect of additives on behavior of alkali metals during straw combustion. *J. Zhejiang Univ.* **2006**, *40*, 599–604.
33. He, F.; Wei, F.J.; Ma, C.J.; Zhao, H.; Fan, Y.; Wang, L.; Wang, J. Performance of an intelligent biomass fuel burner as an alternative to coal-fired heating for tobacco curing. *Pol. J. Environ. Stud.* **2020**, *30*, 131–140. [[CrossRef](#)]
34. Xu, Y.; Zhang, H.; Yang, F.; Tong, L.; Yan, D.; Yang, Y.; Wu, Y. Experimental investigation of pneumatic motor for transport application. *Renew. Energy* **2021**, *179*, 517–527. [[CrossRef](#)]
35. Yu, D.; Ma, Z.; Wang, R. Efficient smart grid load balancing via fog and cloud computing. *Math. Probl. Eng.* **2022**, *2022*, 3151249. [[CrossRef](#)]